Post-fire residual capacity of protected and unprotected concrete filled steel hollow columns.

POST-FIRE RESIDUAL CAPACITY OF PROTECTED AND UNPROTECTED CONCRETE FILLED STEEL HOLLOW COLUMNS

David I. Rush*, Luke A. Bisby* and Allan Jowsey**

* BRE Centre for Fire Safety Engineering, School of Engineering, University of Edinburgh, UK
e-mails: d.rush@ed.ac.uk, luke.bisby@ed.ac.uk

** International Paint Ltd., Gateshead, UK
e-mail: allan.jowsey@akzonobel.com

Keywords: Concrete filled steel hollow sections, CFS, Post-fire residual strength, Intumescent coatings.

Abstract. *Concrete filled steel hollow structural (CFS) sections are an increasingly popular means to support large compressive loads in buildings. Whilst the response of unprotected CFS sections during a fire is reasonably well researched, their post-fire residual structural performance is less well established. The results of 19 post-fire residual eccentric axial compression tests on unprotected and protected CFS columns is presented, along with six unheated control tests. The tests confirm that as the maximum exposed temperature within the cross-section increases, the residual strength capacity, ductility and axial-flexural stiffness decrease. The data presented herein can be used to assess the ability to predict the residual capacity of CFS columns after fires using available post-fire structural and material models.*

1 INTRODUCTION

Concrete filled steel hollow structural sections (CFS) are hollow steel sections in-filled with plain or reinforced concrete to provide superior load carrying capacity and structural fire resistance as compared with unfilled steel tubes. CFS sections are an attractive, efficient, and sustainable means by which to carry large compressive loads in multi-storey buildings. The concrete infill and the steel tube work together at ambient temperatures, during a fire, and after a fire; the steel tube acts as stay-in-place formwork during casting of the concrete, thus reducing forming and stripping costs, and provides a smooth, rugged, architectural surface finish. The concrete infill enhances the tube's resistance to local buckling, and is further confined by the steel tube, thus slightly increasing the load bearing capacity of the concrete.

Whilst structural fire resistance design guidance is available [1] for CFS columns, after a fire when a building may have not experienced a major structural failure, a question arises as to the level of damage that may have been sustained and whether (and also how) the building can be safely repaired. Relatively little work is available on the post-fire residual strength of fire-exposed CFS columns.

This paper presents tests on the post-fire residual compressive load bearing and lateral deformation capacity of 19 CFS columns after being exposed to fire (notably, in an unloaded condition) and cooled to ambient temperature prior to structural testing to failure; six unheated control columns are also tested.

2 BACKGROUND

Han and colleagues have previously presented tests and analysis of CFS columns after fire exposure, including post-fire material models for prediction CFS columns' capacity [2] and more than 20 post-fire residual tests [2, 3] on both protected and unprotected CFS columns. Han's work considers only the ISO 834 fire curve, with tests on square and circular columns ranging in length between 380 and 1200 mm and cross-section size between 80 and 133 mm. Wall thicknesses between 2.9 and 4.8 mm were considered. Han et al.'s steel tubes were filled with plain concrete ranging in strength from 35 to 72 MPa.

Unprotected specimens were heated for 90 mins whilst protected specimens were heated for 180 mins, with two thirds of the columns loaded concentrically. Eccentrically loaded columns had initial load eccentricities of 15 to 18 mm and unsurprisingly failed at lower loads than identical concentrically loaded columns.

Han et al.'s work demonstrated that the residual mechanical behaviour of the fire exposed columns under axial load was 'ductile,' and it was also shown that composite enhancement (i.e. confinement) of the concrete core remained present after heating [3]. The post-heated columns failed in either global buckling or local buckling, with accompanying crushing of the concrete core. The fire duration, column section size, and slenderness ratio were observed to have significant effects on the residual strength of the columns, whereas other parameters (steel ratio, concrete strength, and steel strength) had only minor effects. Unsurprisingly, loss of strength was considerably less for protected sections [4]. Interestingly, it was noted that load eccentricity appeared to be important for the *residual strength index* of the columns.

Table 1. Testing matrix and maximum temperatures recorded in steel tube and concrete core during fire testing.

Test specimen[a]	Size (mm)	Wall thick. (mm)	Infill type[b]	Heating regime[c]	F.R.[d]	Temperatures (°C)[e]			
						Steel	Conc. face	35 mm	Conc. cent.
S13FNN		**10**	**FIB**	**N**	**N/A**	**20**	**20**	**20**	**20**
S11FNN		**5**	**FIB**	**N**	**N/A**	**20**	**20**	**20**	**20**
S13FIN		10	FIB	I	N/A	991	969	893	886
S11FIN	**120**	5	FIB	I	N/A	979	930	856	841
S11FSN		*5*	*FIB*	*S*	*N/A*	*988*	*956*	*833*	*826*
S11FIC		5	FIB	I	90	314	290	281	281
S11FSC		*5*	*FIB*	*S*	*90*	*434*	*383*	*319*	*322*
C11HNN		**5**	**HSC**	**N**	**N/A**	**20**	**20**	**20**	**20**
C11FNN		**5**	**FIB**	**N**	**N/A**	**20**	**20**	**20**	**20**
C12FNN		**8**	**FIB**	**N**	**N/A**	**20**	**20**	**20**	**20**
C13FNN		**10**	**FIB**	**N**	**N/A**	**20**	**20**	**20**	**20**
C13FIN		10	FIB	I	N	1005	995	924	871
C12FIN		8	FIB	I	N	992	977	913	888
C11HIN	**139.7**	5	HSC	I	N	996	952	835	822
C11FIN		5	FIB	I	N	997	954	834	820
C11FSN		*5*	*FIB*	*S*	*N*	*980*	*935*	*787*	*773*
C13FIC		10	FIB	I	90	375	358	350	349
C12FIC		8	FIB	I	90	389	387	373	361
C11HIC		5	HSC	I	90	348	337	319	317
C11FIC		5	FIB	I	90	403	397	380	340
C11FSC1		*5*	*FIB*	*S*	*90*	*380*	*375*	*368*	*366*
C11FIC.14d	139.7	5	FIB	I	90	404	371	365	365
C11FIC.28d		5	FIB	I	90	470	452	435	432
C11FIC.75		5	FIB	I	75	608	542	509	514
C11FIC.120		5	FIB	I	120	620	579	568	514

[a]*Shape (where S = square and C = circular sections) – size – wall thickness – fill type – fire exposure – protection type (- special test)*, [b]FIB = fibre reinforced concrete, HSC = high strength concrete, [c]I = ISO 834, S = smouldering fire, N = unheated, [d]F.R. = fire resistance design rating, [e]ave. max. temp. at TCs

3 EXPERIMENTAL PROGRAMME

The current testing program involved eccentric axial compressive loading, to failure, of 25 CFS columns; details of the full testing program are given by Rush [5], and an overview is provided in Table 1. Nineteen of the specimens were heated for two hours (or more) prior to structural testing to assess their residual response, whilst the remaining six were used as unheated control specimens. Five parameters were assessed: (1) cross-section shape, (2) steel tube wall thickness, (3) type of infill concrete, (4) applied fire curve, and (5) presence of applied protection. Four additional tests were also performed to evaluate

the impacts of (6) concrete age at the time of testing, and (7) intumescent coating thickness. Seven square (S1) and 18 circular (C1) sections were tested with various steel wall thicknesses (5, 8 or 10 mm). The steel tubes were 1400 mm in length and were made from Grade S355 steel. The tubes were filled with ready-mix high strength (70 MPa compressive strength) concrete (HSC) or fibre reinforced concrete (FIB). The FIB mix differed from the HSC mix only in that it incorporated hybrid steel and polypropylene fibre reinforcement at of 45 kg/m^3 and 2 kg/m^3, respectively. Fifteen of the columns were exposed to an ISO 834 (*I*) fire [6] and four were exposed to the Eurocode smouldering (slow-growth) fire (*S*) [7]. Eight columns were unprotected and 11 were protected with a thin film intumescent coating sold under the trade name Interchar 1120 (trade name stated only for factual accuracy).

Temperatures within the cross sections during fire exposure were recorded at two vertical sections (at approximately *L/3* and *2L/3*) using K-Type thermocouples (TCs), as shown in Figure 1. All heated columns were exposed to the fire for 120 minutes as outlined in Table 1 (except in one case where the protection was designed to give 120 minutes fire resistance and the test was continued for 180 minutes), after which point the specimens were allowed to cool within the furnace for a further two hours before the furnace doors were opened. The intumescent coating thicknesses for the protected CFS sections were prescribed using current UK guidance, with a presumed steel tube limiting temperature of 520^{o}C and required fire resistance of 90 minutes (apart from two specimens where the fire resistance was designed for 75 minutes or 120 minutes, respectively).

The details, dimensions, and material properties of the specimens outlined in Table 1 were selected to ensure that the ambient capacity of the CFS columns was less than the 2000 kN maximum load capacity of the available structural testing equipment. Full details of the fire tests are given, along with full and detailed descriptions of the effectiveness of the intumescent fire protection coating, by Rush [5]. For the current paper the key issue is the maximum temperature experienced at various locations within the column cross-sections; these are also given in Table 1.

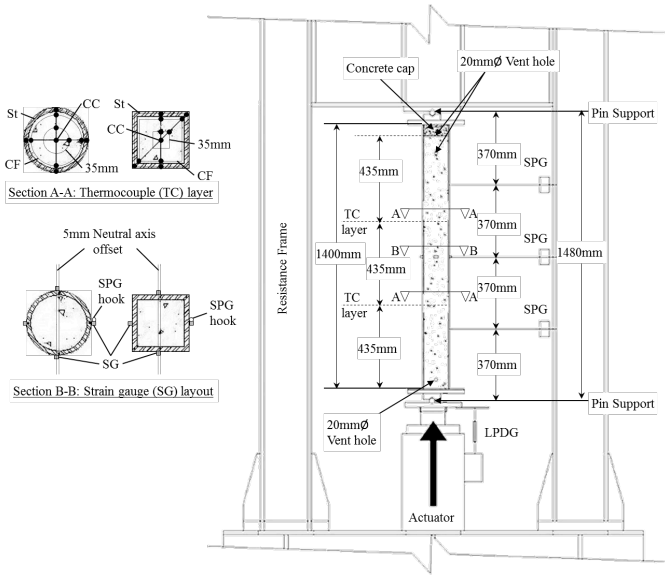

Figure 1. Schematic of tests set up and specimen details for residual capacity tests.

3.1 Test procedure

During structural testing the columns were attached to pin supported plates at either end, through which a small axial eccentricity of 5 mm was introduced to the compressive load; this also controlled the

direction of lateral deflection and aided with lateral deflection measurements. The 5 mm eccentricity also agrees with design guidance for structural imperfections (effective length/300). The columns were inserted into a self-reacting structural frame, as shown in Figure 1, with an effective buckling length of 1480 mm. Bonded foil stain gauges (SGs) were installed on the steel tube evenly around the columns' perimeters at their mid-height (Section B-B in Figure 1); two in line with the pin supports and two perpendicular to the pin supports. Three string pot displacement gauges (SPGs) were attached at the columns at their quarter heights to measure lateral deformations. A linear potentiometer displacement gauge (LPDG) measured axial displacement (stroke) of the hydraulic jack used load the columns, and a pressure gauge was attached in-line with an electric hydraulic power pack to record load. Tests were manually controlled using an approximate actuator stroke rate of 2.5 to 3.5 mm/min, and were terminated when the rotation of the top or bottom plate was impeded by the plates attached to the actuator or frame.

4 RESIDUAL CAPACITY TEST RESULTS

Selected results are given in Table 2, including the: observed failure load (N_{test}); axial deflection at failure (δ_y); mid-span lateral deflection at failure (δ_{x2}); and average axial strain at mid-height at failure. Table 2 also gives the observed failure mode and the pre-failure axial stiffness of the columns, measured between applied loads of 200 and 400 kN and based on the average axial strain at mid-height.

Table 2. Observed loads, deflections, and strains at failure, failure type, and pre-failure axial stiffness for residual tests.

	Test data[a]						RSI[b]	
	N_{test} [1]	δ_y [2]	δ_{x2} [3]	ε_{ave} [4]	Failure[5]	k_{cfs} (kN/mm)[6]	N_{FNN} [7]	N_{test} /N_{FNN}
S13FNN	**1949**	**15.7**	**-8.2**	**-2393.7**	**G**	**127.1**	**1949**	**1.00**
S11FNN	**1467**	**14.4**	**-4.7**	**-2687.5**	**LB**	**103.5**	**1467**	**1.00**
S13FIN	1082	10.3	-3.7	-625.2[c]	G	113.6	1949	0.56
S11FIN	617	8.0	-3.7	-4343.9	G	90.2	1467	0.42
S11FSN	*576*	*7.7*	*-3.8*	*-1960.2*	*G*	85.3	*1467*	*0.39*
S11FIC	1243	12.9	-4.2	-1513.8	LB	107.9	1467	0.85
S11FSC	*1215*	*13.3*	*-4.9*	*-1587.3*	*LB*	97.4	*1467*	*0.83*
C13FNN	**1772**	**15.7**	**-10.0**	**-2700.4**	**G**	**137.1**	**1772**	**1.00**
C12FNN	**1664**	**14.8**	**-10.0**	**-2869.9**	**G**	**112.3**	**1664**	**1.00**
C11FNN	**1372**	**13.4**	**-8.3**	**-1760.9**	**G - LB**	**121.6**	**1372**	**1.00**
C11HNN	**1346**	**14.6**	**-10.2**	**-3051.2**	**G**	**90.8**	**1346**	**1.00**
C13FIN	1061	9.7	-3.7	-991.7	G	121.4	1772	0.60
C12FIN	813	8.6	-3.4	-1010.7	G	108.4	1664	0.49
C11FIN	583	10.3	-4.2	-3988.2	G	65.9	1372	0.42
C11HIN	591	7.4	-4.0	-1115.6	G	91.4	1346	0.44
C11FSN	*601*	*7.6*	*-5.2*	*-1566.1*	*G*	96.4	*1346*	*0.45*
C13FIC	1241	11.0	-4.8	-1213.6	G	122.6	1772	0.70
C12FIC	1285	12.8	-5.8	-2105.7	G - LB	113.6	1664	0.77
C11HIC	1192	13.4	-12.5	-3378.8	G - LB	109.1	1346	0.89
C11FIC	714	9.6	-5.8	-1536.5	LB - G	94.5	1372	0.52
C11FSC	*795*	*9.6*	*-3.9*	*-2081.2*	*LB - G*	100.4	*1372*	*0.58*
C11FIC.14d	764	8.9	-5.3	-1359.7	LB - G	104.3	1346	0.57
C11FIC.28d	741	9.2	-4.3	-1630.5	LB - G	92.0	1346	0.55
C11FIC.75	833	12.5	-13.9	-3120.9	G	96.7	1346	0.62
C11FIC.120	835	11.2	-8.9	-2498.7	G	95.2	1346	0.62

[a]Results at failure for; [1]load, [2]axial deflection, [3]mid-height lateral deflection, [4]average strain, and [5]failure mode (G = global buckling, LB = local buckling), and [6]pre-failure axial stiffness; [b]RSI = residual strength index, with [7]$N_{FNN} = N_{test}$; [c]strain gauge failure.

4.1 Overall response

As expected, elevated temperature exposure affected the observed axial failure load (N_{test}), the axial stiffness (k_{cfs}), and both axial deflections (δ_y) and lateral deflections (δ_{x2}). For instance, the axial failure

loads for unheated, fire-exposed but protected, and fire-exposed and unprotected columns decreased with exposure to increasingly severe maximum temperatures. Similarly, the reduction of k_{cfs} and axial deflections at failure as exposure temperatures increased is clear. Columns failed in either global buckling (GB) or local buckling (LB). In most cases a global buckling mode occurred first and resulted in the formation of a local buckle close to column mid height, however in some cases the local buckle formed away from the column mid height (typically near the top of the column) before global buckling initiated. Comparatively lower failure loads were observed in the columns that failed due to local buckling as compared with those that initially displayed a global buckling deformed shape. Specific reasons for the different failure modes are not clear, and no obvious trends were apparent in the failure mode test data.

The *residual strength index* (defined as the ratio of the tested strength to the strength of an identical unheated column; RSI = N_{test}/N_{FNN}) shows that the fire protection reduced the loss of strength to between 10% and 40%, this being an improvement of about 30% as compared to unprotected sections. The RSI was also dependent on the size of the steel tube wall, with thicker walls retaining more strength.

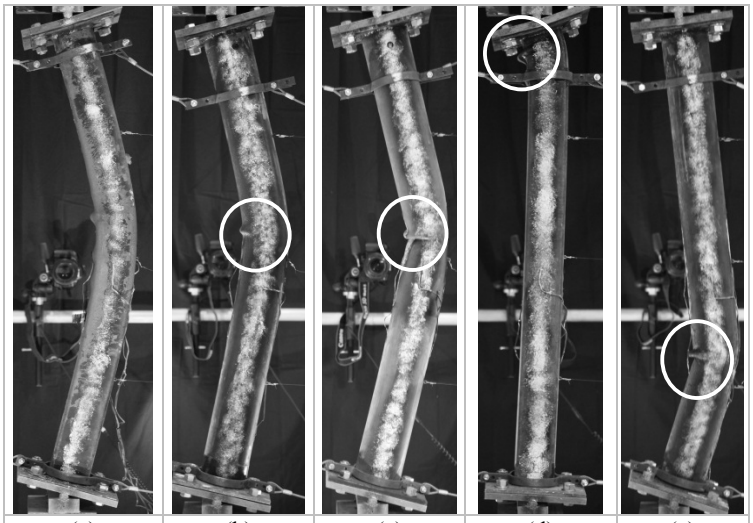

(a) S11FIN	(b) C11FNN	(c) C11FIC.28d	(d) S11FNN	(e) C11FIC

Figure 2. Typical deflected shapes and observed failure modes: (a) global buckle; (b) global buckle with local buckling; (c) mid-height local buckle; (d) local buckle at top; and (e) local buckle at quarter height.

4.2 Failure modes

A representative selection of the various failure modes and post failure deflected shapes that were observed are shown in Figure 2. Circular sections failed either by: (1) global buckling as in Figure 2(a); (2) local buckling as in Figure 2(c); or (3) global buckling leading to local buckling of the steel tube as in Figure 2(b). Global buckling failure modes (1) and (3) were observed in all tests of circular sections apart from C11FIC, C11FSC, C11FIC.14d, and C11FIC.28d, all of which were protected, 5 mm wall thickness columns in which failure was by local buckling at approximately the third-height of the column as shown in Figure 2(e). The reason for the local buckling failures could be due to small voids being present within the concrete core as a result of the problems during the initial casting of the concrete (this is strongly suspected by the authors), or may simply be coincidental.

Local buckling was observed in square section tests S11FIC, S11FSC, and S11FNN, all with 5 mm wall thickness, in the region of required moisture venting holes near the tops of the steel tubes, as shown in Figure 2(d). This may be due to the reduced cross-sectional area of steel at this location leading to

stress concentrations, initiating failure. Unprotected fire-exposed columns S11FI(/S)N and S13FIN failed in global buckling as the concrete core in these columns had a much lower residual strength. Thus, the residual axial/flexural stiffness of these columns was insufficient to prevent global buckling before the steel yielded around the vent holes. Test S13FNN could not be failed in the testing rig (limited to 2000 kN); however, a global buckling failure mode was observed to be initiating at the maximum load.

5 EFFECTS OF COLUMN PARAMETERS

5.1 Steel tube thickness

Figures 3(a), (b), and (c) show observed load versus axial and load versus lateral deflection responses for C11FI(/N)x (5 mm steel thickness), C12FI(/N)x (8 mm thick), C13FI(/N)x (10 mm wall thickness) CFS sections. As the wall thickness increased the observed failure load and pre-failure axial stiffness also increased, as expected. All sections failed in global buckling apart from C11FIC, which failed in local buckling at the third height of the column. This local buckling failure mode resulted in different load-deflection and load-strain response as compared to those observed during global buckling failure. Figures 3(e) and (f) showed a similar comparison for square cross-section columns. For both shapes, columns with larger steel wall thickness generally experienced greater retention of mechanical properties after fire (other factors being equal).

5.2 Concrete infill type

Figures 3(a) and (d), show load-deflection and load-strain relationships for C11xxx columns filled with either FIB or HSC infill, respectively. The effect of the type of concrete infill had no obvious effect on the load deflection relationships for CFS columns. The only significant change in response is seen by comparing C11FIC and C11HIC, where load versus deflection was markedly different; however this is thought to be due to the different failure modes experienced by C11FIC and C11HIC; these being local buckling failure and global buckling failure, respectively (the reasons for which remain unknown).

5.3 Concrete age and protection thickness

Figure 3(g) shows the load-deflection response for the two specimens that were exposed to fire after 14 days (C11FIC.14d) and 28 days (C11FIC.28d) after concrete casting, to evaluate the impact of the age of the infill concrete (primarily on the thermal response and the effectiveness of the intumescent fire protection during furnace testing). The load-deflection for these two columns were similar to those observed for C11FIC (see Figure 3(a)) since all three columns experienced local buckling failure modes at their third height. Due to the presence of local buckling of the column, other generalizations are difficult to make.

Figure 3(g) also shows the load-deflection response for the two specimens that had dry film thicknesses (DFTs) designed and applied on the basis of required fire resistance times of 75 minutes (C11FIC.75) and 120 minutes (C11FIC.120), respectively. Both of these columns failed in global buckling and achieved similar maximum temperatures throughout their cross-sections. Thus, similar load-deflection and load-strain relationships were observed. A similar response was seen for C11HIC (see Figure 3(d)), which had a DFT designed for 90 minutes fire resistance and also failed by global buckling, however lower temperatures were experienced in C11HIC, and it was stiffer and retained more strength.

5.4 Thermal insult

Figures 3(a) and (e) show the load-deflection response for the C11FSx and S11FSx sections exposed to the smouldering fire [7]. Similar responses were seen as compared to the identical sections exposed to the ISO 834 fire [6], with similar local buckling failure modes for the protected (xxxxxC1) sections and global buckling failure modes for the unprotected (xxxxxN) sections. No obvious differences in response were evident based on the heating curve; this is because similar maximum temperatures were experienced for both types of thermal insult, indicating that the intumescent fire protection performed similarly under both the standard [6] and slow-growth [7] heating curves.

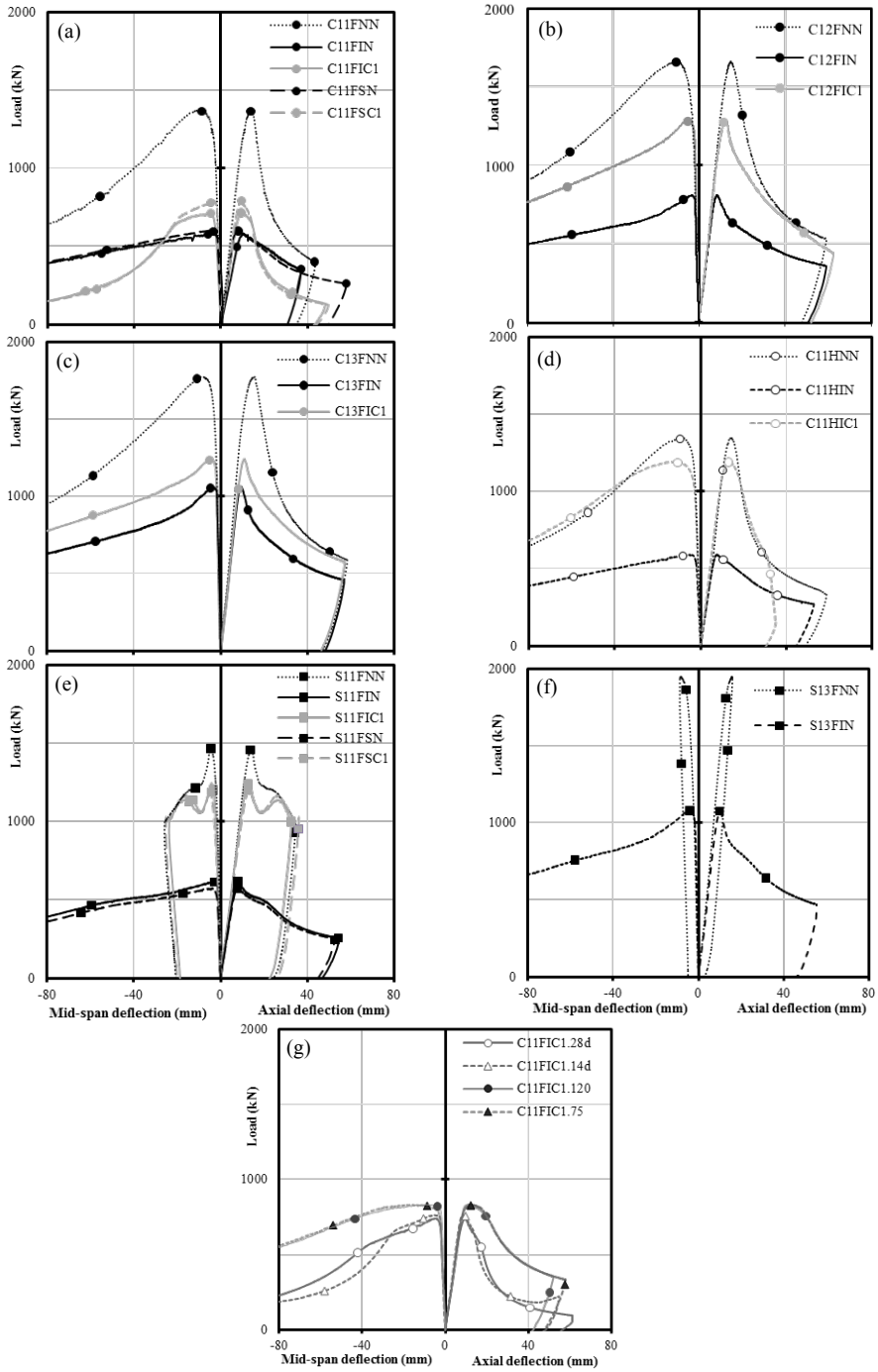

Figure 3. Load versus lateral deflections at mid-height (left), or axial deflections (right), for; (a) C11Fxx; (b) C12Fxx; (c) C13Fxx, (d) C11Hxx, (e) S11Fxx, (f) S13Fxx, and (g) C11FIC.xx columns.

5.5 Cross-section shape

Comparison of figures 3(a) and (e) or figures 3(c) and (f) shows the influence of cross-section shape on the load-deflection response for S1xxxx square sections as opposed to C1xxxx columns. The response of the unprotected S1xFIN sections is similar to that seen for the unprotected C1xFIN circles, with global buckling failure modes being observed in these cases. The response of the S11FNN and S11FIC sections was markedly different to any of the other columns; these square sections failed locally at the top of the columns where the cross-sectional area was reduced due to the presence of vent holes in the steel hollow sections, as already noted. Thus, cross-sectional shape appears to influence performance due to the formation of alternative failure modes and this issue should be considered in generating design guidance.

6 CONCLUSIONS

A series of 25 residual strength tests were conducted on CFS columns that had undergone different severities of heating in furnace tests due to the type of thermal insult applied or thr use of intumescent fire protection. The residual tests showed that as the temperatures within the CFS sections increased, the residual axial failure load and axial stiffness of the CFS columns decreased. This is clearly due to the reduction in strength and stiffness of both the steel and concrete due to elevated temperature exposure. It was also observed that protected columns, in which much lower maximum temperatures were experienced due to the protection from the intumescent coatings, retained up to 30% more of their ambient structural capacity compared to the unprotected columns, where the residual strength of the column was as low as 40% of the ambient capacity after 120 minutes of fire exposure. The columns failed either by global or local buckling. For the circular sections local buckling was only observed in the sections with 5 mm wall thicknesses and where the severity of the temperatures experienced in the cross-section were reduced by the presence of intumescent coatings. For the square sections local buckling was observed when the section had not been exposed to fire. The load-deflection and load-strain relationships of different CFS columns were found to be similar, depending on the failure mode experienced. The data presented herein are being used by the authors to assess the ability to predict the residual capacity of CFS columns after fires, using available post-fire structural and material models.

7 ACKNOWLEDGEMENTS

We gratefully acknowledge support from Arup (Fire), The Ove Arup Foundation, The Royal Academy of Engineering, the Engineering and Physical Sciences Research Council, and the School of Engineering at the University of Edinburgh, part of the Edinburgh Research Partnership in Engineering.

REFERENCES

[1] CEN, *BS EN 1994-1-1*, European Committee for Standardization, Brussels, Belgium, 2004.

[2] Han, L.H. and Huo, J.S., “Concrete filled hollow structural steel columns after exposure to ISO-834 standard fire”, *Journal of Structural Engineering*, 129(1), 68, 2003.

[3] Han, L.H., Huo, J.S. and Wang, Y.C., “Compressive and flexural behaviour of concrete filled steel tubes after exposure to standard fire”, *Journal of Constructional Steel Research*, 61(7), 882–901, 2005.

[4] Han, L.H., Yang, Y.F., Yang, H. and Huo, J.S., Residual strength of concrete-filled RHS columns after exposure to the ISO-834 standard fire. *Thin-Walled Structures*, 40(12), 991–1012, 2002.

[5] Rush, D., *Fire performance of unprotected and protected concrete filled structural hollow sections*, PhD Thesis, University of Edinburgh, 2013.

[6] ISO, *ISO 834*, International Organization for Standardization, Geneva, Switzerland, 1999.

[7] CEN. *BS EN 13381-8*, European Committee for Standardization, Brussels, Belgium, 2010.